

## Effect of glass fiber on the electrical resistivities of polyoxymethylene/maleic anhydride-grafted polyethylene/multiwalled carbon nanotube composites

Bo-Yuan Zhang,<sup>1</sup> Ling Xu,<sup>1</sup> Zhao-Xia Guo,<sup>1</sup> Jian Yu,<sup>1</sup> Satoshi Nagai<sup>2</sup>

<sup>1</sup>Key Laboratory of Advanced Materials (MOE), Department of Chemical Engineering, Tsinghua University, Beijing 100084, People's Republic of China

<sup>2</sup>Mitsubishi Engineering-Plastics Corporation, 5-6-2 Higashiyawata, Hiratsuka, Kanagawa 254-0016, Japan

Correspondence to: Z.-X. Guo (E-mail: guozx@mail.tsinghua.edu.cn) and J. Yu (E-mail: yujian03@mail.tsinghua.edu.cn)

**ABSTRACT:** The effect of glass fiber (GF) on the electrical resistivities of polyoxymethylene (POM)/maleic anhydride-grafted polyethylene (MAPE)/multiwalled carbon nanotube (MWCNT) composites is investigated. The POM/MAPE/MWCNT composites at a MWCNT loading of 0.75% are nonconductive because most of MWCNTs are isolated in the MAPE islands, and their electrical resistivities decrease significantly after the addition of GF because of the formation of MAPE-coated GF structure, which facilitates the formation of conductive paths and was confirmed by field emission scanning electron microscopy (FESEM). The formation of MAPE-coated GF structure is attributed to the interaction between GF and MAPE during melt compounding, as contrasted by the uncoated GF using high-density polyethylene (HDPE) instead of MAPE. Nonconductive POM/5–20% MAPE/0.75% MWCNT composites become conductive upon the addition of 20% GF. This preparation method for conductive materials can be generalized to POM/5–20% maleic anhydride-grafted polypropylene (MAPP)/0.75% MWCNT composites. © 2014 Wiley Periodicals, Inc. *J. Appl. Polym. Sci.* 2015, 132, 41794.

**KEYWORDS:** blends; composites; fibers; graphene and fullerenes; nanotubes

Received 9 July 2014; accepted 22 November 2014

DOI: 10.1002/app.41794

### INTRODUCTION

Electrically conductive polymer composites are widely used in many fields such as in shielding of electromagnetic interference and electrostatic dissipation, and have many advantages such as wide range of conductivity, easy processing, and diversity of polymer matrix and conductive fillers.<sup>1–3</sup> Carbon nanotubes (CNTs) are nowadays one of the most commonly used carbon fillers. They show higher electrically conductive efficiency as compared with traditional carbon fillers: carbon black (CB), carbon fiber (CF), and graphite.<sup>4,5</sup>

Using polymer blends as the matrices to prepare conductive composites has attracted much attention ever since the first report on the concept of double percolations published by Sumita *et al.* in 1991.<sup>6–8</sup> The electrical conductivities of carbon filler filled-polymer blends can be significantly improved compared to those of carbon filler filled-single polymers because of the selective localization of the carbon filler in a continuous polymer phase or at the interfaces of the blends.<sup>6–14</sup> However, when the carbon filler is selectively localized in the dispersed phases, the materials are usually nonconductive because the

conductive paths cannot be formed with carbon fillers isolated in the islands, unless the particle sizes are very small and the interparticle distances are small enough to allow tunneling effect to happen.<sup>15–17</sup> The localization of the carbon filler depends on both thermodynamic (interfacial energy) and kinetic factors (such as viscosity, mixing time, and mixing sequence).<sup>6–15,18–22</sup>

Polyoxymethylene (POM) is one of the most useful engineering plastics because of its excellent properties such as high tensile strength, high rigidity, creep, and chemical resistance. When MWCNTs are filled in POM-based blends, most CNTs are localized in the other polymer phase such as MAPE, maleic anhydride-grafted polypropylene (MAPP), thermoplastic polyurethane (TPU), and polyamide 6 (PA 6), which have higher polarity and thus higher affinity to CNTs than POM, and the materials usually have lower electrical conductivity as compared with CNT-filled POM. A literature survey has shown that the addition of GF can increase the conductivity of CB-filled polymer blends where CB is selectively localized in the dispersed phase by forming coated-GF structure.<sup>23–25</sup> Narkis *et al.*<sup>23,24</sup> added GF to PP/PA66/CB system where CB is localized in the minor PA66 phase, and found that conductive materials can be

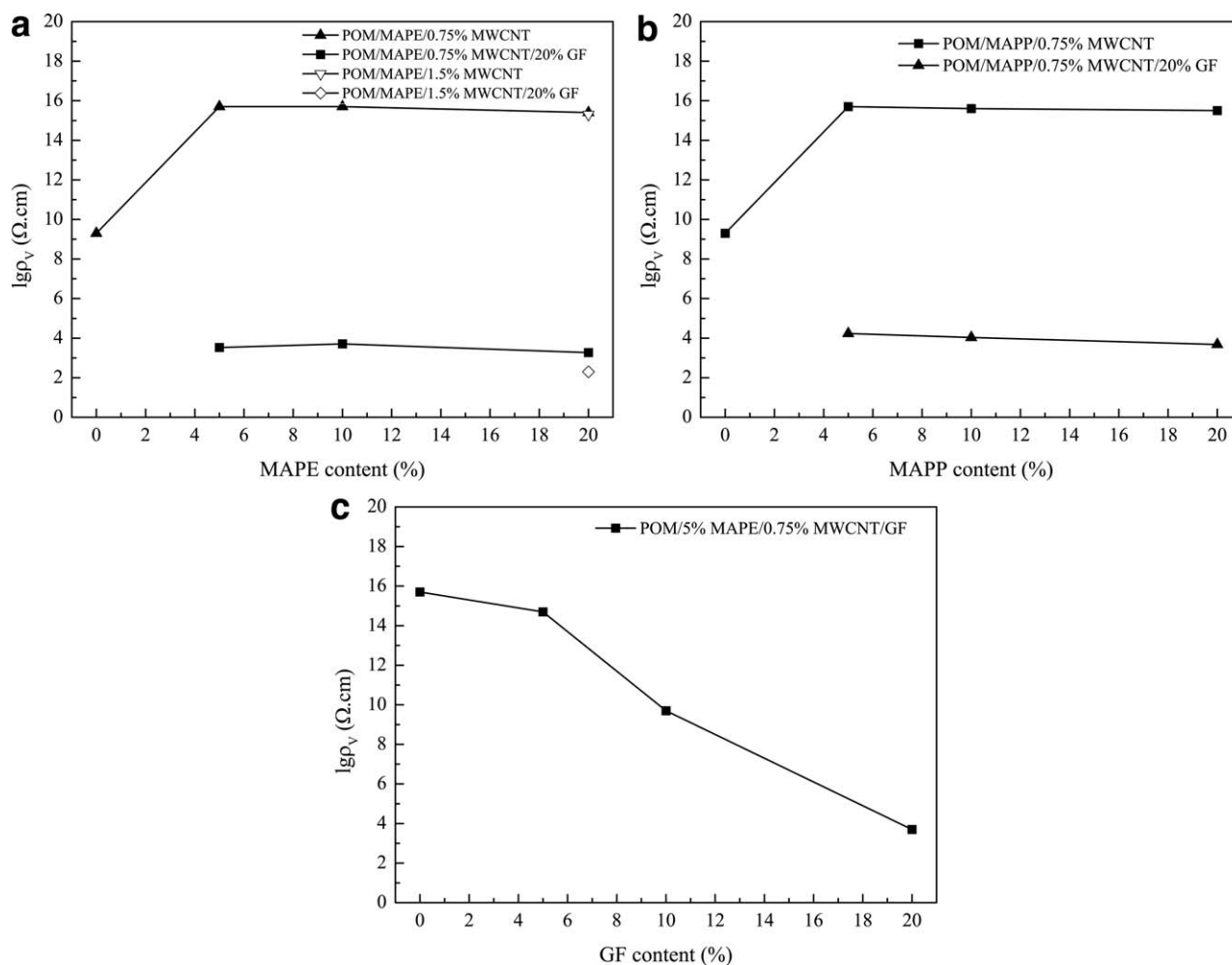


**Figure 1.** Effects of GF on electrical resistivities of (a) POM/MAPE/MWCNT, (b) POM/MAPP/MWCNT, and (c) POM/5%MAPE/0.75% MWCNT composites.

obtained at much lower CB content by forming PA66-coated GF structure. They attributed the increased conductivity to the formation of a triple percolation morphology of a continuous GF network, continuous PA66 phase and continuous CB paths. Li *et al.*<sup>25</sup> reported improved conductivity of PP/epoxy/CB composites with the addition of GF through the construction of epoxy-coated GF structure. By adopting this idea, we envisage constructing similar kind of structure in CNT-filled POM-based blends by addition of GF in order to improve the electrical conductivity.

In this work, the effect of amino-functionalized GF on the electrical resistivity of POM/MAPE/MWCNT composites is investigated. MAPE-coated GF structure is evidenced by FESEM, and the mechanism for increased conductivity is explained.

## EXPERIMENTAL

### Materials

The MWCNTs with a density of 50–100 kg/m<sup>3</sup> were supplied by Tsinghua University (Beijing, China). The purity of MWCNTs was about 95 wt %, the average diameter was 10 nm, and the length was less than 10 μm. The POM with a density of 1.41 g/cm<sup>3</sup> was

provided by Yuntianhua (Yunnan, China). The GF (ECS 305K), with a length of 4.5 mm and amino groups (the atomic concentration of N is 2.36% as measured by XPS) on the surface, was provided by Chongqing Polycomp International (Chongqing, China). The MAPE and MAPP were prepared in our laboratory.<sup>26</sup> The HDPE (5200B) was provided by SINOPEC Beijing Yanshan Company (Beijing, China).

### Sample Preparation

POM/MAPE (or MAPP)/MWCNT and POM/MAPE (or MAPP)/MWCNT/GF composites were prepared by melt mixing in a torque rotational rheometer (RM-200A Rheometer, Harbin Hapro Electrical Technology). The mixing temperature was 200°C, the rotation speed was 60 rpm, and the mixing time was 5 min. All the contents of MAPE, MAPP, MWCNTs and GF are wt % to the whole composite.

### Characterizations

To measure the electrical resistivity, the composites were compressed into plates using a hot press for 5 min. The hot press temperature was 190°C, and the pressure was 8 MPa. Samples with a diameter of 75 mm and a thickness of 0.375 mm or a diameter of 30 mm and a thickness of 2.5 mm were prepared

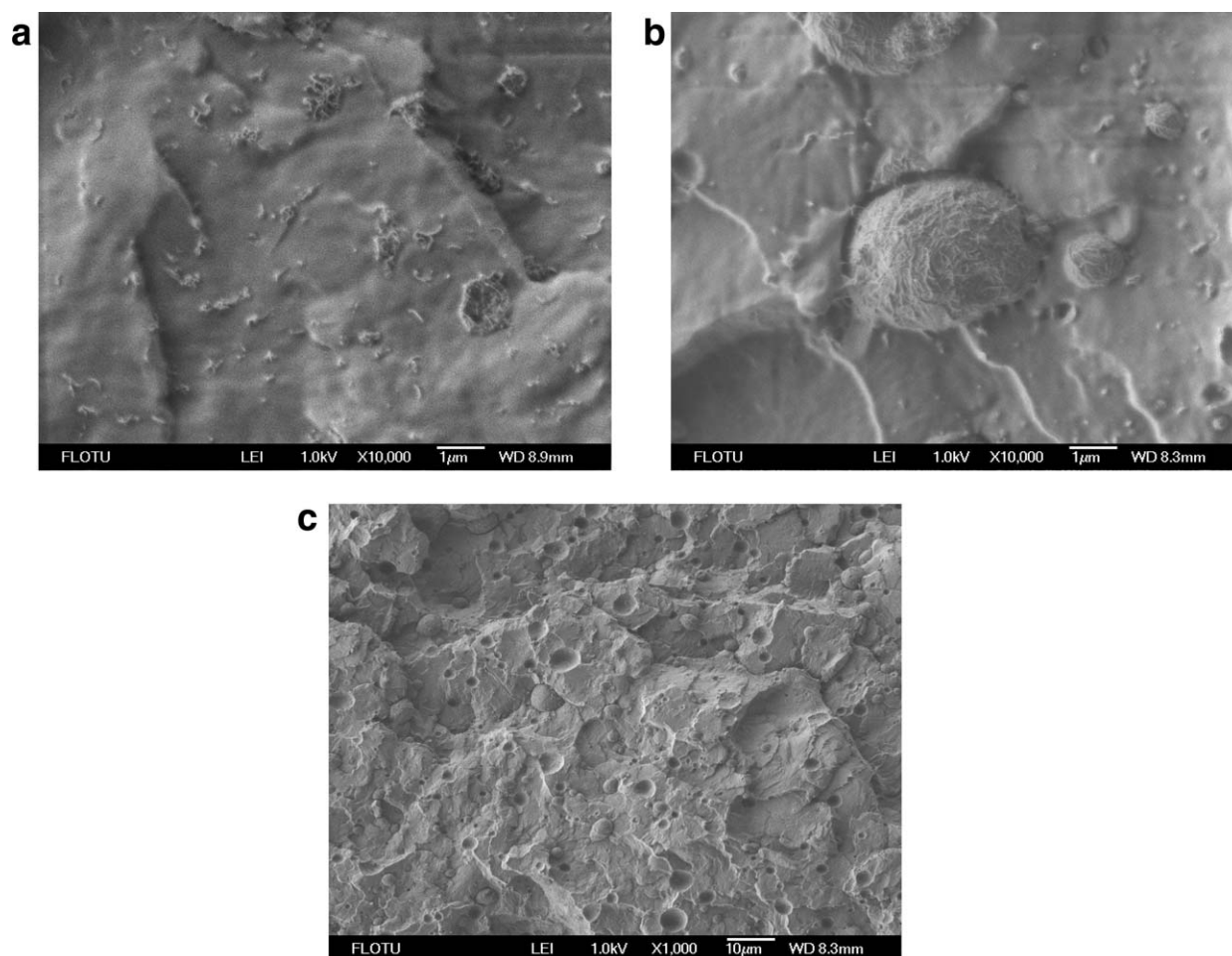


**Figure 2.** FESEM micrographs of (a) POM/0.75% MWCNT and (b, c) POM/5% MAPE/0.75% MWCNT composites.

for high or low electrical resistivity measurements, respectively. Samples with electrical resistivity of  $>10^8 \Omega \text{ cm}$  were measured by ZC-36 Resistivity Test (Shanghai Cany Precision Instrument). The test voltage is set for 250, 100, or 10 V, depending on the resistance of the sample, and the current is read on panel. The electrical resistivity is calculated using the formula:  $\rho_V = \pi V d^2 / 4 I L$ , where  $V$  is the voltage,  $I$  is the current,  $d$  is the diameter of the sample, and  $L$  is the thickness. Samples with electrical resistivity of  $<10^5 \Omega \text{ cm}$  were measured by KDY-1 Resistivity Test (Guangzhou Kunde Technology).<sup>18</sup> The principle of the low resistivity test is based on the four-point method with constant current source. All the reported electrical resistivities are volume resistivities. Data for high and low resistivity are averages of two and four measurements, respectively. Deviations of all the measurements are within 5%.

To investigate the morphology of the composites, the hot compressed samples were cryo-fractured in liquid nitrogen and then characterized by FESEM (JEOL model JSM-7041 instrument).

The X-ray photoelectron spectroscopy (XPS) data of GF were obtained using an ESCALab220i-XL electron spectrometer (VG Scientific Instruments).

The Fourier transform infrared (FTIR) spectra of samples in the form of KBr pellets were characterized by Thermo-Nicolet 6700 FTIR spectrometer with signal averaging 64 scans at a resolution of  $4 \text{ cm}^{-1}$ .

The optical microscopy graphs were obtained using a Nikon Type 104 optical microscope with a JVC color video camera.

## RESULTS AND DISCUSSION

### Effect of GF on the Electrical Resistivities of POM/MAPE/MWCNT Composites

The electrical resistivities of POM/MAPE/MWCNT and POM/MAPE/MWCNT/GF composites as a function of MAPE content are shown in Figure 1(a). The contents of MWCNTs and GF were fixed at 0.75% and 20%, respectively, and the contents of MAPE were 5, 10, and 20%. The electrical resistivity of POM/MWCNT composites significantly increases with the addition of MAPE and approaches the electrical resistivity of the POM matrix. After adding GF, the electrical resistivity of POM/MAPE/MWCNT composites sharply decreases from  $10^{16}$  to  $10^4 \Omega \text{ cm}$ . This indicates that the addition of GF could effectively improve the electrical conductivity of the POM/MAPE/MWCNT composites. The electrical resistivity of the POM/MAPE/MWCNT/GF

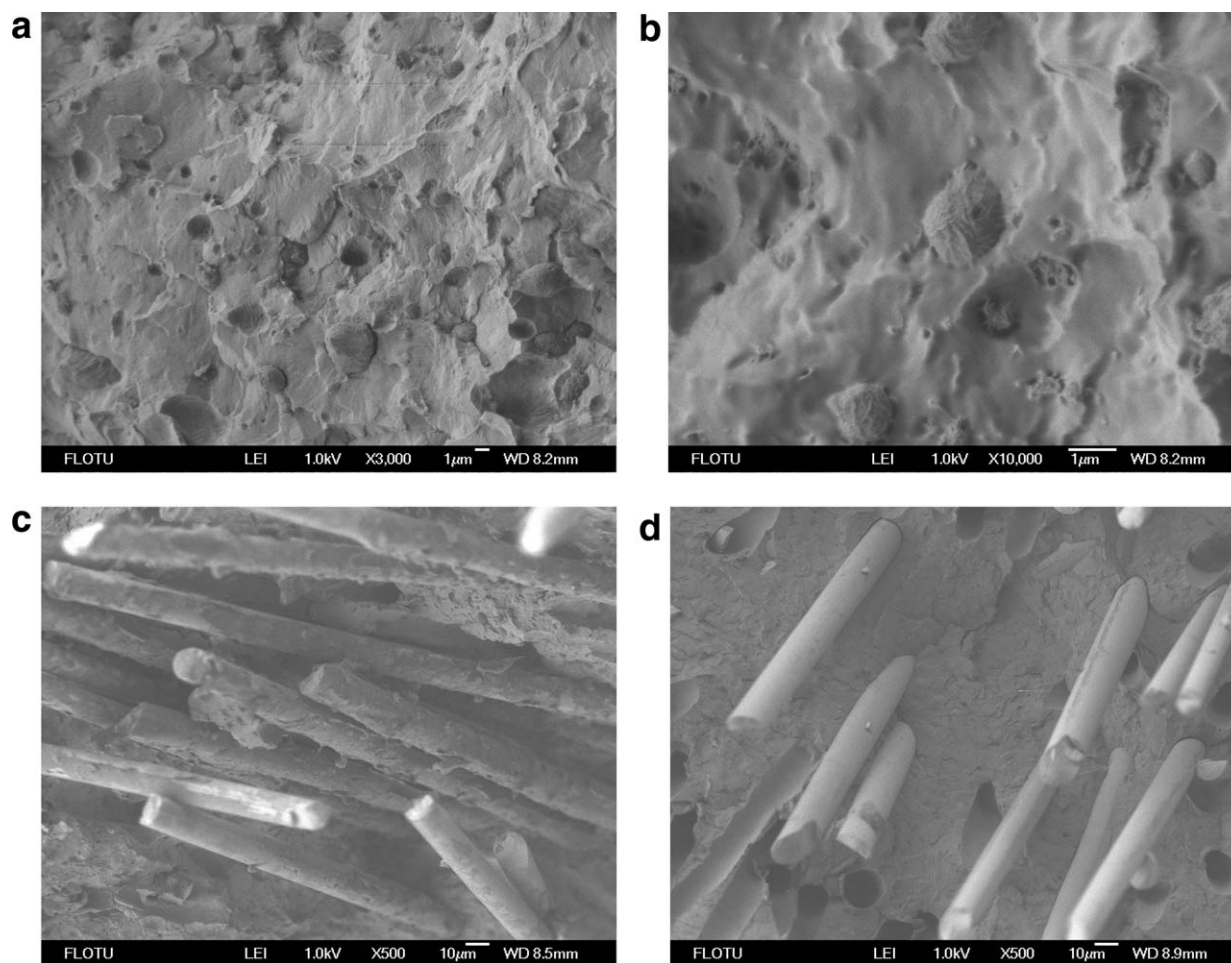


**Figure 3.** FESEM micrographs of (a–c) POM/5% MAPE/0.75% MWCNT/20% GF and (d) POM/0.75% MWCNT/20% GF composites.

composites has no obvious change with the increase in MAPE content. When MWCNT content increases to 1.5%, the electrical resistivity of POM/20% MAPE/1.5% MWCNT composite decreases from  $10^{15}$  to  $10^{2.5}$   $\Omega$  cm after the addition of 20% GF, showing similar effect on the electrical

resistivity of the composite. Compared to POM/20% MAPE/0.75% MWCNT/20% GF composite, POM/20% MAPE/1.5% MWCNT/20% GF composite has an order lower electrical resistivity, indicating improved electrical conductivity with more MWCNTs.

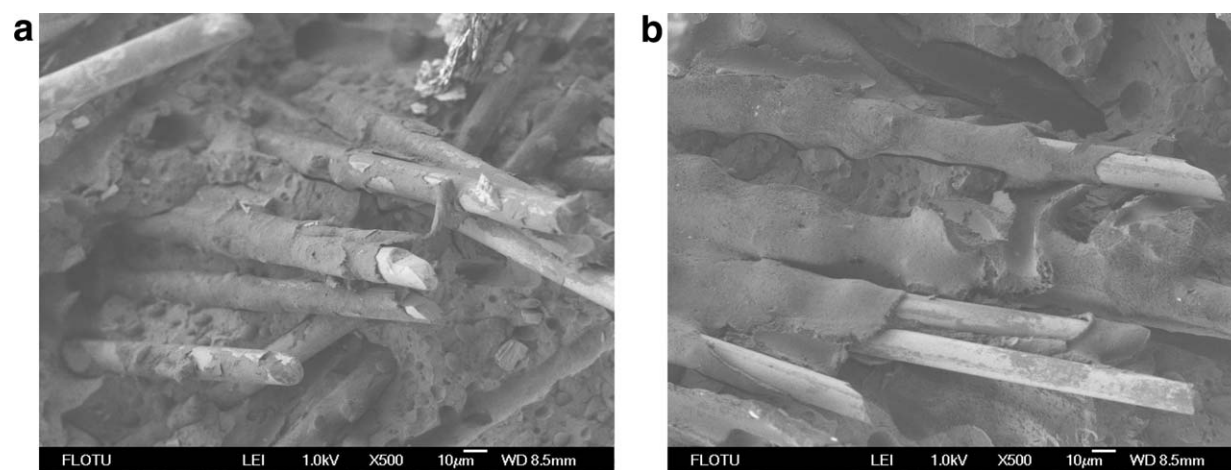


**Figure 4.** FESEM micrographs of POM/MAPE/0.75% MWCNT/20% GF composites at different MAPE contents: (a) 10% and (b) 20%.

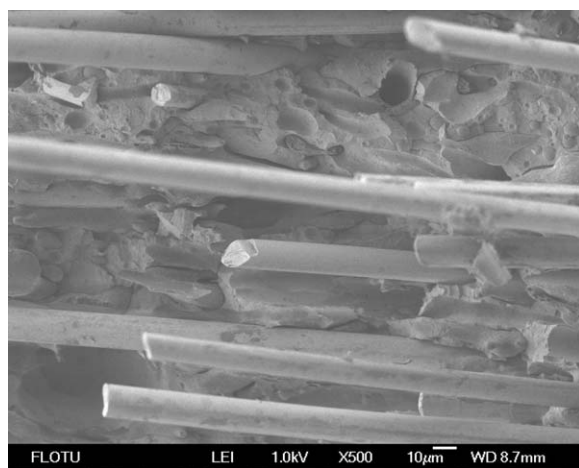


**Figure 5.** FESEM micrograph of POM/20% HDPE/0.75% MWCNT/20% GF composites.

### Morphology of the Electrically Conductive Composites

POM-based materials can hardly be characterized by TEM due to the low stability of POM under high-power electron beam. So in this work, the morphology of all the POM-based composites was characterized by FESEM. Figure 2 shows FESEM micrographs of POM/5% MAPE/0.75% MWCNT composite along with that of POM/0.75% MWCNT composite for comparison. In POM/0.75% MWCNT composite [Figure 2(a)], MWCNTs disperse uniformly in POM matrix. Some MWCNTs appear as a single nanotube, while some MWCNTs exist as small aggregates. A typical sea-island structure was observed in POM/5% MAPE/0.75% MWCNT system with POM as the continuous phase and MAPE as the dispersed phase. The size of the dispersed phase is in micrometer scale [Figure 2(b,c)]. Comparing Figure 2(b) to Figure 2(a), which was taken at the same magnification and the same MWCNT content, only few MWCNTs are observed in the POM matrix phase in Figure 2(b), and most MWCNTs are localized in the dispersed MAPE phase. This seems reasonable considering the high polarity of anhydride group of MAPE. MWCNTs have more affinity to MAPE than to POM. The distance among the dispersed MAPE particles is a few micrometer, far bigger than 10 nm to allow tunneling effect to happen,<sup>27</sup> therefore the electrical resistivity of POM/5% MAPE/0.75% MWCNT composite is high up to  $10^{16} \Omega \text{ cm}$  [Figure 1(a)]. When MAPE content increases to

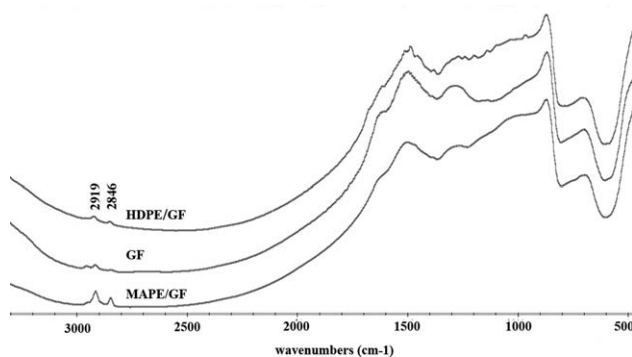


**Figure 6.** FTIR spectra of extracted HDPE/GF, MAPE/GF, and GF.

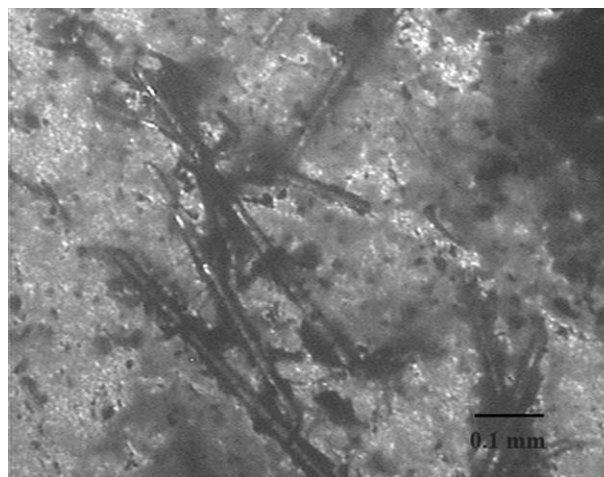


**Figure 7.** Optical Microscopy graph of GFs isolated from POM/MAPE/MWCNT/GF composite.

10 and 20%, the morphology is similar to the case of 5% MAPE unless the sizes of MAPE particles are much bigger. Since most MWCNTs are localized in the MAPE particles, the conductive paths cannot be formed, and thus the materials are nonconductive.

The morphology of POM/5% MAPE/0.75% MWCNT/20% GF composite is shown in Figure 3. Again, a sea-island structure is observed and only few MWCNTs are observed in the POM matrix phase [Figure 3(a,b)]. GFs are coated with a layer of polymer, which is considered to be MAPE [Figure 3(c)], because POM cannot wet GF as shown in the case of POM/0.75% MWCNT/20% GF composite where the surfaces of GFs are smooth [Figure 3(d)]. The morphology of the POM/MAPE/0.75% MWCNT/20% GF composites is similar with more MAPE contents (10 and 20%). The most significant difference is the thickness of the coating layer, which increases with MAPE content, as evidenced in Figure 4(a,b).

From the above observation, it can be confirmed that MAPE can effectively coat on GF surface. Since HDPE cannot coat GF (Figure 5), the interaction between GF and MAPE must play an important role in the formation of MAPE-coated GF structure. To confirm the existence of the interaction between GF and MAPE, HDPE/GF, and MAPE/GF (weight ratio is 1 : 1) composites were prepared by melt mixing under similar conditions to the case of POM/MAPE/GF/MWCNT composites and characterized by FTIR. No obvious difference was observed between the two samples. Therefore, HDPE/GF, MAPE/GF, and GF were extracted using Soxhlet extractor with xylene for 48 h and then refluxed in xylene for 5 times (1 h/time, fresh xylene was used in each time) to remove unbonded polymer (HDPE and MAPE). The extracted HDPE/GF, MAPE/GF, and GF were characterized by FTIR (Figure 6). Neither the characteristic peak of anhydride groups nor that of amide groups (the reaction product) is observed in the spectrum of MAPE/GF, because of their small contents and the broad peak of GF at the interested region. It is noted that the  $\text{CH}_2$  peaks at  $2919$  and  $2846 \text{ cm}^{-1}$  are weak in GF and HDPE/GF, but it is much stronger in MAPE/GF, indicating a certain amount of MAPE is tightly bounded on the surface of GF through covalent bonding<sup>28</sup> and/or hydrogen bonding

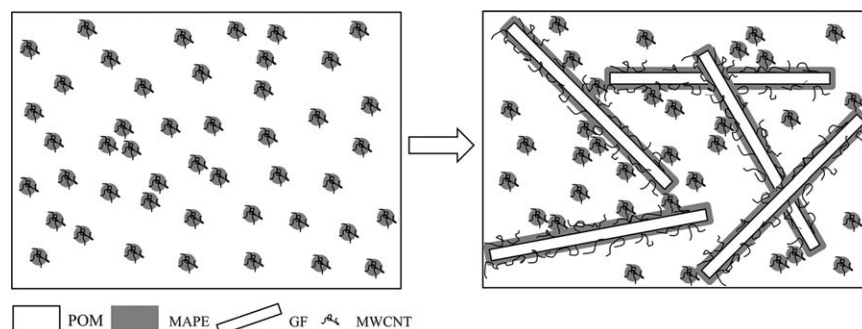


**Figure 8.** Illustration of POM/MAPE/MWCNT composites (left) and the formation of conductive network in POM/MAPE/MWCNT/GF composites (right).

between the amino groups of GF and the anhydride groups of MAPE. This confirms the interaction between MAPE and GF.

Although coating of GF by MAPE is thermodynamically favored by the interaction between GF and MAPE, kinetic factors also affect the coating process. Because the melt viscosity of MAPE is relatively high, it is reasonable that some parts of the huge

surface area of GF are not covered by MAPE as observed from Figures 3(c) and 4.

To investigate whether fracture of GFs happens during melt mixing, the lengths of GFs after melt mixing were measured by optical microscopy (Figure 7) after removing POM by extracting with hexafluoroisopropanol. The average length of 200 GFs is 0.53 mm. Although GFs shorten after melt mixing (as compared to the original length of 4.5 mm), they are still much longer than MWCNTs (10  $\mu\text{m}$ ). In other words, GFs are long enough to act as long distance charge transporters and to facilitate construction of conductive network.

#### Mechanism for the formation of Conductive Paths

It can be concluded from the above results that the addition of GF is an effective way to construct conductive network and improve the conductivity of POM/MAPE/MWCNT composites through the formation of MAPE-coated GF structure. The mechanism for the formation of conductive paths is illustrated in Figure 8. In the system, there are two types of MWCNT-containing species: MAPE-coated GFs and MAPE particles, which are clearly evidenced in Figure 4(a) where MAPE-coated GFs appears as long fibers and MAPE particles as quasi-spheres. They form cosupporting conductive networks in which MAPE-coated GFs act as long distance charge transporters and MAPE particles serve as an interconnection between the coated GFs, similar to the cases of mixed carbon filler-filled polymers such as CB/MWCNT-filled PP<sup>29</sup> and graphite/CF-filled HDPE.<sup>30</sup> The role of GF is twofold: first, the use of GF can increase the effective volume of MAPE because MAPE-coated GF acts as a type of conducting species, which has a much bigger volume than that of its corresponding MAPE coating; Second, when GF is added to the system, less POM is used by design, and this can increase the effective concentration of the conducting species.

To verify the universality of the effect of GF on the construction of conductive network, POM/MAPP/MWCNT/GF composites were also investigated, as shown in Figures 1(b) and 9. In accordance with the expectation, the addition of GF can also improve the electrical conductivity of POM/MAPP/MWCNT composites by forming MAPP-coated GF structure. This suggests that GF can increase the electrical conductivity of MWCNT-filled POM-based blends as long as the second polymer can interact with the amino-functionalized GF during melt compounding, i.e., using functional polymer as the second

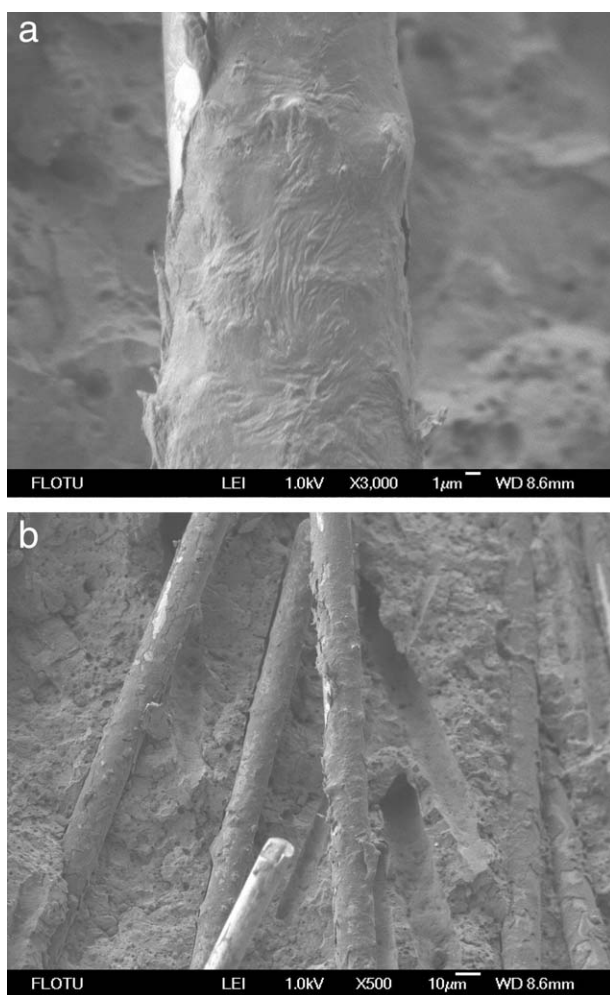


**Figure 9.** FESEM micrographs of POM/5% MAPP/0.75% MWCNT/20% GF composites.

polymer could be a way to obtain MWCNT-filled conductive POM-based polymer blends.

#### Effect of GF Content on the Electrical Resistivity of POM/MAPE/MWCNT/GF Composite

The electrical resistivity of POM/MWCNT/MAPE/GF composite as a function of GF content is shown in Figure 1(c). The contents of MAPE and MWCNTs were fixed at 5% and 0.75%, respectively. The electrical resistivity of the composite gradually decreases with the increase in GF content. The system becomes percolated at about 20% GF, which is comparable with the results obtained in the work of Narkis *et al.*<sup>23,24</sup> and Li *et al.*,<sup>25</sup> where GF was used to improve the electrical conductivity of PP/PA66/CB and PP/epoxy/CB composites by forming PA66- and epoxy-coated GF structure. As discussed above, MAPE-coated GFs play the role of long distance charge transporters in the formation of conductive paths, therefore, with increasing GF content, the conductive paths are easier to form and the electrical resistivity of the sample decreases.

#### CONCLUSIONS

The enhancement of electrical conductivity of POM/MAPE/MWCNT composites is achieved by the addition of GF having amino groups on the surface due to the formation of MAPE-coated GF structure. The interaction between the amino-functionalized GF and MAPE during melt compounding is important for the formation of MAPE-coated GF structure, because using nonreactive HDPE instead of MAPE cannot form coated structure. Adding 20% GF to nonconductive POM/5–20% MAPE/0.75% MWCNT composites can lead to conductive materials. The mechanism for the conduction is attributed to the formation of cosupporting conductive networks in which MAPE-coated GFs act as long distance charge transporters and MAPE particles serve as an interconnection between the coated GFs. Using MAPP instead of MAPE gives similar electrical resistivity data, showing versatility of the method. The addition of GF is an efficient way to improve the electrical conductivity of MWCNT-filled POM-based blends.

#### ACKNOWLEDGMENTS

The authors thank the Beijing Key Laboratory of Green Reaction Engineering and Technology (Department of Chemical Engineering, Tsinghua University) for kindly providing the MWCNTs.

#### REFERENCES

1. Zhang, W.; Dehghani-Sani, A. A.; Blackburn, R. S. *J. Mater. Sci.* **2007**, *42*, 3408.
2. Strumpler, R.; Glatz-Reichenbach, J. *J. Electroceram.* **1999**, *3*, 329.
3. Chung, D. *Carbon* **2001**, *39*, 279.
4. Bauhofer, W.; Kovacs, J. Z. *Compos. Sci. Technol.* **2009**, *69*, 1486.
5. Spitalsky, Z.; Tasis, D.; Papagelis, K.; Galiotis, C. *Prog. Polym. Sci.* **2010**, *35*, 357.
6. Sumita, M.; Sakata, K.; Asai, S.; Miyasaka, K.; Nakagawa, H. *Polym. Bull.* **1991**, *25*, 265.
7. Sumita, M.; Sakata, K.; Hayakawa, Y.; Asai, S.; Miyasaka, K.; Tanemura, M. *Colloid. Polym. Sci.* **1992**, *270*, 134.
8. Zhang, C.; Han, H. F.; Yi, X. S.; Asai, S.; Sumita, M. *Compos. Interfaces.* **1999**, *6*, 227.
9. Gubbels, F.; Jerome, B.; Teyssie, P.; Vanlathem, E.; Deltour, R.; Calderone, A.; Parente, V.; Bredas, J. L. *Macromolecules* **1994**, *27*, 1972.
10. Gubbels, F.; Blacher, S.; Vanlathem, E.; Jerome, R.; Deltour, R.; Brouers, F.; Teyssie, P. *Macromolecules* **1995**, *28*, 1559.
11. Thongruang, W.; Balik, C. M.; Spontak, R. J. *J. Polym. Sci. Part B: Polym. Phys.* **2002**, *40*, 1013.
12. Potschke, P.; Bhattacharyya, A. R.; Janke, A. *Polymer* **2003**, *44*, 8061.
13. Goldel, A.; Kasaliwal, G.; Potschke, P. *Macromol. Rapid Commun.* **2009**, *30*, 423.
14. Goldel, A.; Marmur, A.; Kasaliwal, G. R.; Potschke, P.; Heinrich, G. *Macromolecules* **2011**, *44*, 6094.
15. Xiong, Z. Y.; Sun, Y.; Wang, L.; Guo, Z. X.; Yu, J. *Sci. China Chem.* **2012**, *55*, 808.
16. Xu, Z. B.; Zhao, C.; Gu, A. J.; Fang, Z. P. *J. Appl. Polym. Sci.* **2007**, *103*, 1042.
17. Li, J.; Fang, Z. P.; Tong, L. F.; Gu, A. J.; Liu, F. *J. Appl. Polym. Sci.* **2007**, *106*, 2898.
18. Fenouillot, F.; Cassagnau, P.; Majeste, J. C. *Polymer* **2009**, *50*, 1333.
19. Sun, Y.; Guo, Z. X.; Yu, J. *Macromol. Mater. Eng.* **2010**, *295*, 263.
20. Sun, Y.; Jia, M. Y.; Guo, Z. X.; Yu, J.; Nagai, S. *J. Appl. Polym. Sci.* **2011**, *120*, 3224.
21. Xiong, Z. Y.; Zhang, B. Y.; Wang, L.; Yu, J.; Guo, Z. X. *Carbon* **2014**, *70*, 233.
22. Xiong, Z. Y.; Wang, L.; Sun, Y.; Guo, Z. X.; Yu, J. *Polymer* **2013**, *54*, 447.
23. Narkis, M.; Lidor, G.; Vaxman, A.; Zuri, L. *IEEE Trans. Electron Packag. Manufact.* **2000**, *23*, 239.
24. Narkis, M.; Lidor, G.; Vaxman, A.; Zuri, L. *J. Electrostat.* **1999**, *47*, 201.
25. Li, Y.; Wang, S. F.; Zhang, Y.; Zhang, Y. *J. Appl. Polym. Sci.* **2005**, *98*, 1142.
26. Wang, L.; Guo, Z. X.; Yu, J. *J. Appl. Polym. Sci.* **2011**, *120*, 2261.
27. Fiuschau, G. R.; Yoshikawa, S.; Newnham, R. E. *J. Appl. Phys.* **1992**, *72*, 953.
28. Chow, W. S.; Abu Bakar, A.; Mohd Ishak, Z. A.; Karger-Kocsis, J.; Ishiaku, U. S. *Eur. Polym. J.* **2005**, *41*, 687.
29. Sun, Y.; Bao, H. D.; Guo, Z. X.; Yu, J. *Macromolecules* **2009**, *42*, 459.
30. Thongruang, W.; Spontak, R. J.; Balik, C. M. *Polymer* **2002**, *43*, 2279.